Scientia Pharmaceutica

ÖSTERREICHISCHE PHARMAZEUTISCHE GESELLSCHAFT

MDPI

Article

Structural Characterization and Cytotoxic Effects of Bioactive Compounds Isolated from *Caulerpa sertularioides* Against Human Cancer Cell Lines

Edgar Sandoval-Petris [1,2], Rosalio Ramos-Payan [1], Hisila del Carmen Santacruz-Ortega [3], Maribel Plascencia-Jatomea [4], María Guadalupe Burboa-Zazueta [2], Idalia Osuna-Ruíz [5], Elsa Maribel Aguilar-Medina [1] and Carmen María López-Saiz [4,*]

1 Facultad de Ciencias Químico Biológicas, Universidad Autónoma de Sinaloa, Culiacán C.P. 80013, Mexico; edgar.sandoval@unison.mx (E.S.-P.); rosaliorp@uas.edu.mx (R.R.-P.); maribelaguilar@uas.edu.mx (E.M.A.-M.)
2 Departamento de Investigaciones Científicas y Tecnológicas, Universidad de Sonora, Hermosillo C.P. 83000, Mexico; maria.burboa@unison.mx
3 Departamento de Investigación en Polímeros y Materiales, Universidad de Sonora, Hermosillo C.P. 83000, Mexico; hisila.santacruz@unison.mx
4 Departamento de Investigación y Posgrado en Alimentos, Universidad de Sonora, Hermosillo C.P. 83000, Mexico; maribel.plascencia@unison.mx
5 Unidad Académica de Ingeniería en Biotecnología, Universidad Politécnica de Sinaloa, Mazatlán C.P. 82199, Mexico; iosuna@upsin.edu.mx
* Correspondence: carmen.lopezsaiz@unison.mx

Abstract

Compounds isolated from the macroalga *Caulerpa sertularioides* have been reported to exhibit cytotoxic activity. The objective of this study was to assess the antioxidant effects of compounds isolated from *C. sertularioides* as well as their antiproliferative effect against cancerous cell lines and to elucidate their chemical structure. The antiproliferative activity of *C. sertularioides* extracts was evaluated using the MTT standard assay in cancerous and non-cancerous cell lines. Morphological changes were observed via fluorescence microscopy, and the chemical structure of bioactive compounds was determined by nuclear magnetic resonance. Antioxidant activity was assessed using ABTS and DPPH methods. Among all extracts, the acetone extract exhibited the highest antioxidant activity (IC_{50} of 27.3 ± 6.1 µg/mL) in the ABTS assay, which classifies it as a very potent antioxidant. Among the tested extracts, the hexane extract showed the strongest antiproliferative activity in breast (MDA-MB-231) and cervical cancer (HeLa) cell lines. The most active fraction (F15), obtained by open-column chromatography of hexane extract, exhibited the highest bioactivity against the MDA-MB-231 cell line (IC_{50} of 55 ± 3.1 µg/mL); these cells exhibited morphological changes consistent with apoptosis. NMR analysis revealed signals tentatively assigned to 1-monolinolein, glycerol, bis(2-ethylhexyl) phthalate and bis(2-ethylhexyl) terephthalate. These findings support the potential of *C. sertularioides* as a source of bioactive compounds with antioxidant and antiproliferative properties.

Keywords: antiproliferative activity; selectivity index; apoptosis; bioactive compound

Academic Editor: Yulin Ren

Received: 21 April 2026
Revised: 25 August 2026
Accepted: 31 August 2026
Published: 9 September 2026

1. Introduction

Cancer is a disease characterized by dysregulated control of cell proliferation [1]. This disease is a global public health problem and a leading cause of death. In 2024, nearly 10 million deaths were attributed to this disease worldwide [2], and it is estimated

that the number of new cases and deaths will increase in the coming years [3]. The most common types of cancer are breast, lung, colon and rectum, prostate, skin, and stomach [4]. Cancer treatment faces several obstacles, including side effects (cardiotoxicity, nephrotoxicity, myelosuppression, neurotoxicity, hepatotoxicity, gastrointestinal toxicity, mucositis, alopecia) [5] and the development of drug resistance (influenced by genetic, epigenetic, proteomic, metabolic, or microenvironmental factors) [6].

In recent decades, progress has been made in the search for new anticancer strategies emphasizing treatment efficacy while reducing side effects [7] and drug resistance, incorporating various strategies, such as combination drug therapy, anti-angiogenic therapy, allosteric drug therapies, nanomedicine, and traditional medicine [8]. Particular attention has also been directed toward naturally occurring chemopreventive and chemotherapeutic agents. These natural molecules generally act at multiple levels and targets, including transcription factors, cytokines, adhesion molecules, growth factor receptors, and inflammatory enzymes [9].

Due to the wide variety of species and diverse microenvironments, marine species have been the subject of multiple investigations in the search for promising natural molecules that could exhibit anticancer activity [10]. Several marine species such as sponges, starfish, bryozoans, tunicates, sea cucumbers, slugs, bacteria, cyanobacteria, and algae have been investigated for new bioactive compounds with anticancer potential [11]. Research aimed at the search for new drugs has also extended to marine algae from the three major groups: Ochrophyta (brown algae), Rhodophyta (red algae), and Chlorophyta (green algae) [12]. Within this context, the green alga *Caulerpa sertularioides* has drawn attention due to its rich phytochemical profile, which includes anticancer compounds such as fatty acids, alkaloids, carotenoids, chlorophylls, phenolic compounds, sterols, glycoproteins, polysaccharides, sulfolipids, and terpenoids [13–15]. Supporting this potential, it has been reported that methanol extracts from *C. sertularioides* inhibit telomerase activity in acute lymphoblastic leukemia cell lines [16]. Additionally, polysaccharides extracted from these algae demonstrated iron-chelating activity, suggesting antioxidant properties [17]. Osuna-Ruiz et al. observed a notable antiproliferative effect of acetone extracts of *C. sertularioides* on murine lymphoma cells [18]. Agena et al. found that ethanolic extracts from the same species showed cytotoxic, proapoptotic and anti-invasive effects in a three-dimensional lung cancer cell model [19]. In another study, Sivakumar et al. observed that gold nanoparticles containing *C. sertularioides* aqueous extract induced significant cytotoxic activity against colon cancer [20]. Altogether, these findings highlight *C. sertularioides* as a promising source of compounds with anticancer potential. Therefore, the present study aimed to evaluate the effect of compounds isolated from *C. sertularioides* on the proliferation and morphological changes in human cancer cell lines, assess their antioxidant properties, and elucidate the chemical structure of bioactive molecules.

2. Materials and Methods

2.1. Collection of the Specimen

Caulerpa sertularioides specimens were collected from the beaches of San Carlos, Sonora, Mexico (27°56′29″ N, 111°03′07″ W), in October 2023. The species was identified according to Norris [21], and a voucher specimen was deposited in the herbarium archive of the University of Sonora (ID: Ficoteca-USON #17).

Samples were initially rinsed in situ with seawater to remove excess sand and epibionts and then transported in ice-packed polyethylene bags. In the laboratory, the samples were rinsed with distilled water and subjected to 1 min sonication to eliminate remaining

contaminants. The biomass was then lyophilized, ground into a fine powder, weighed, and stored at −20 °C until further use. The biomass yield was calculated as follows:

$$Biomass\ yield\ (\%) = \frac{mass\ of\ dried\ biomass}{mass\ of\ wet\ biomass} \times 100$$

2.2. Extraction and Isolation of Compounds with Antiproliferative Potential

Bioactive compounds were extracted from *C. sertularioides* following the methodology described by Trujillo-Ruiz et al. [22]. For each independent extraction, 40 g of lyophilized biomass was mixed with hexane at a 1:14 w/v ratio, continuously stirred for 24 h and filtered under vacuum using Whatman No. 1 filter paper (Cytiva, Little Chalfont, Buckinghamshire, UK). The filtrate was concentrated using a rotary evaporator (RE300, Yamato Scientific Co., Ltd., Tokyo, Japan) at 30 °C, followed by final evaporation to dryness under a nitrogen stream. The residual biomass on the filter paper underwent sequential extraction processes with acetone and methanol, using the same procedure. Crude extracts were stored at −20 °C until further analysis. All extractions were performed in triplicate.

After solvent removal, each crude extract was weighed, and the extraction yield was calculated as follows:

$$Extraction\ yield\ (\%) = \frac{mass\ of\ dried\ extract}{mass\ of\ dried\ biomass} \times 100$$

Isolation of bioactive compounds was carried out by gravity-driven open-column chromatography, following the procedure described by Trujillo-Ruiz et al. [22] with modifications. The crude extract showing the highest antiproliferative activity was selected for fractionation. A glass column (2.5 cm i.d., 74 cm length) was packed with silica gel (70–230 mesh; Sigma-Aldrich, St. Louis, MO, USA), previously activated at 100 °C for 24 h. The silica bed was conditioned and packed using 1 L of hexane. After loading the crude extract onto the column, elution was performed using a stepwise gradient of hexane:ethyl acetate, starting at 100:0 and gradually increasing the proportion of ethyl acetate by 2% every 500 mL of mobile phase until reaching 0:100. Eluates were collected in 250 mL portions.

The collected eluates were monitored by thin-layer chromatography (TLC), using silica gel plates and hexane–ethyl acetate mixtures as mobile phase. Chromatographic spots were visualized under short- and long-wavelength UV light. The retention factor was calculated according to the following equation:

$$Rf = \frac{Cd}{Mpd} \quad (1)$$

where Rf is the retention factor, Cd is the distance traveled by compound (cm), and Mpd is the distance traveled by the mobile phase (cm). Eluates with similar Rf values were grouped and considered the same fraction.

After pooling eluates with similar TLC profiles, each fraction was evaporated to dryness, weighed, and its recovery yield was calculated relative to the mass of crude extract loaded onto the column.

Following the biological evaluation of the chromatographic fractions, the fraction selected for further chemical characterization was subjected to an additional purification step using gravity-driven open-column chromatography. A glass column (1 cm i.d.) was packed with silica gel to a bed height of 9 cm. The selected fraction was loaded onto the column and eluted using a stepwise gradient of hexane:ethyl acetate at the following proportions: 80:20, 77:23, 70:30, 60:40, 50:50, 40:60, and 30:70 (v/v). Eluates were collected sequentially in 5 mL portions, yielding a total of 35 subfractions. Each subfraction was

analyzed by UV–Vis spectroscopy, and its absorption profile was compared with those of the parent fraction and a commercial reference standard. Subfractions with similar UV–Vis profiles were pooled, evaporated to dryness under a nitrogen stream, and subsequently analyzed by NMR.

2.3. Antioxidant Activity

To evaluate the antioxidant activity of the extracts, two radical scavenging assays were conducted, 2,2-diphenyl-1-picrylhydrazyl (DPPH) assay and 2′-azino-bis(3-ethylbenzothiazolin-6-sulfonic acid) (ABTS) assay, following the method described by Trujillo-Ruiz et al. [22]. Three independent experiments were conducted, each with four replicates per treatment. The inhibition percentage was calculated using the following formula:

$$\% \, inhibition = \frac{1 - AbS}{AbC} \times 100 \quad (2)$$

where

AbS—sample absorbance;

AbC—negative control absorbance.

The half-maximal inhibitory concentration (IC_{50}) was determined by plotting inhibition versus extract concentration. Results were expressed in Trolox equivalents, using a standard curve ranging from 0 to 800 µM Trolox.

2.3.1. ABTS Radical Cation Scavenging Assay

A solution containing 3.3 mg of ABTS in 5 mL of distilled water was mixed with potassium persulfate ($K_2S_2O_8$, 3.84 mg/mL) at a 1:1 (v/v) ratio and allowed to react for 16 h in the dark at room temperature. Crude extracts were tested at different concentrations (15.6, 31.2, 62.5, 125, 250, and 500 µg/mL). For each assay, 900 µL of the ABTS reagent with an absorbance of 0.8 and 100 µL of sample were combined and incubated for 30 min. Absorbance was read at 734 nm using a GENESYS 10S spectrophotometer (Thermo Fisher Scientific, Waltham, MA, USA). Antioxidant capacity was expressed as µM Trolox equivalents per gram of extract.

2.3.2. DPPH Radical Scavenging Assay

Extracts were evaluated at the same concentrations described above. For each tube, 900 µL of the DPPH solution (0.06 mg/mL prepared in methanol) with an absorbance of 0.7 and 100 µL of sample were mixed and incubated in the dark at room temperature for 30 min. Absorbance was measured at 540 nm using a GENESYS 10S spectrophotometer (Thermo Fisher Scientific, Waltham, MA, USA). Results were reported as µM Trolox equivalents per gram of extract.

2.4. Cell Lines

This study used five human cancer cell lines, cervical adenocarcinoma (HeLa), colorectal carcinoma (HCT116), invasive breast adenocarcinoma (MDA-MB-231), lung adenocarcinoma (A549), and prostate adenocarcinoma (22Rv1), along with one non-cancerous cell line, retinal pigmented epithelium (ARPE-19); all cell lines were provided by the Cancer Cell Culture Laboratory of the Department of Scientific and Technological Research of the University of Sonora. The cancer cell lines were selected to represent tumors of different tissue origins, including several of the most frequently diagnosed cancers worldwide, such as breast, lung, colorectal, and prostate cancer.

All lines were maintained in Dulbecco's Modified Eagle Medium (DMEM, Sigma-Aldrich, St. Louis, MO, USA) or Roswell Park Memorial Institute (RPMI, Sigma-Aldrich, St. Louis, MO, USA) medium, supplemented with 10% fetal bovine serum (Gibco, Thermo

Fisher Scientific, Grand Island, NY, USA) and antibiotics, and incubated at 37 °C, with 5% CO_2 and 80% humidity.

2.5. Cell Viability Assay

Cell metabolic activity and apparent viability were assessed using the standard MTT assay described by Mosmann [23]. The MTT assay estimates cellular metabolic activity based on the enzymatic reduction of MTT to formazan by metabolically active cells. Therefore, decreases in absorbance were interpreted as reductions in metabolic activity and apparent cell viability rather than as direct evidence of cell death. Briefly, 10,000 cells per well were seeded in a 96-well plate and treated with different crude extracts at two concentrations (100 and 200 µg/mL); two concentrations (100 and 50 µg/mL) were used to evaluate the fractions. After 48 h, 10 µL of MTT reagent (3-(4,5-dimethylthiazol-2-yl)-2,5-diphenyltetrazole bromide) was added and incubated for 4 h. Then, 50 µL of dimethyl sulfoxide (DMSO) was added to dissolve the formazan crystals. Optical density was read using a microplate reader (AD340, Beckman Coulter, Salzburg, Austria) at 570 nm, using 650 nm as the reference wavelength. DMSO, doxorubicin and cisplatin (Cis-diamminedichloroplatinum (II), Sigma-Aldrich, St. Louis, MO, USA) were used as negative and positive controls, respectively. Three independent experiments in triplicate were carried out for each treatment.

2.6. IC_{50} Estimation and Selectivity Index

The half-maximal inhibitory concentration (IC_{50}) was calculated from the linear regression equation based on the percentage of cell viability at different concentrations. This value was used to determine the selectivity index (SI), which indicates the specificity of a compound against cancer cells, as described by Dissanayake et al. [24]. The SI was calculated using the following formula:

$$SI = \frac{IC_{50}\ of\ normal\ cell\ line}{IC_{50}\ of\ cancer\ cell\ line} \quad (3)$$

In the present study, the SI was used as an exploratory comparison between the response of the cancer cell lines and that of the non-cancerous ARPE-19 cell line. Because ARPE-19 cells are not tissue-matched counterparts of the evaluated cancer cell lines, the calculated SI values should not be interpreted as definitive evidence of tumor-specific selectivity.

2.7. Fluorescence Cell Staining and Microscopy Assay

To observe morphological and structural changes induced by the treatment, the method described by Van Vuuren et al. was employed [25]. Briefly, 10,000 cells per well were seeded in 96-well microplates, incubated for 24 h, and then treated with the bioactive fraction at the IC_{50}. After 24 h, cells were fixed with 3.7% formaldehyde in phosphate-buffered saline (PBS) for 15 min, and permeabilized with 0.2% Triton X-100 in PBS for another 15 min.

Cells were stained with phalloidin-tetramethylrhodamine B isothiocyanate (phalloidin, 50 µg/mL) (Sigma-Aldrich, St. Louis, MO, USA) solution to visualize F-actin, and 4′,6-diamidino-2-phenylindole, dilactate (DAPI, 1.5 µg/mL) (Sigma-Aldrich, St. Louis, MO, USA), to stain DNA. Cell morphology was examined using an inverted epifluorescence microscope (DMi8, Leica Microsystems CMS GmbH, Wetzlar, Germany).

2.8. Proton and Carbon Nuclear Magnetic Resonance Analysis

The fractions with the highest biological activity were characterized by nuclear magnetic resonance (NMR) using a Bruker Avance III 400 spectrometer (Bruker BioSpin GmbH, Rheinstetten, Germany). Tetramethylsilane (TMS) was used as the internal reference for both ^{1}H and ^{13}C NMR analyses ($\delta H = 0$ ppm and $\delta C = 0$). The samples were dissolved in deuterated chloroform ($CDCl_3$; Sigma-Aldrich, Saint Louis, MO, USA) at a concentration of 20 mg/mL and transferred to 5 mm NMR tubes. Chemical shifts were reported in parts per million (ppm).

2.9. Statistical Design and Analysis

A completely randomized experimental design was used for cell viability studies. Data are presented as mean ± standard error (SE), based on at least three replicates from three independent experiments. Statistical analyses were performed using analysis of variance (ANOVA), and Tukey's multiple range test was applied to determine significant differences between treatments ($p < 0.05$). All statistical evaluations were conducted using the Minitab 18 statistical package.

3. Results

3.1. Collection, Extraction, and Isolation

The collection of *Caulerpa sertularioides* accounted for a total of 1.34 kg (wet weight). After drying, the sample weight was reduced to 255 g, indicating a moisture content of 81%. After sequential extraction, the highest yields were obtained after extraction with methanol (11.9%), followed by hexane (3%) and acetone (2.3%).

3.2. Antioxidant Activity

The radical scavenging capacity of *C. sertularioides* extracts was evaluated; Table 1 presents the IC_{50} values of *C. sertularioides* extracts obtained using hexane, acetone, and methanol in the ABTS and DPPH radical scavenging assays. The acetone extract exhibited very potent antioxidant activity in the ABTS assay, whereas all other extracts were categorized as weak in the ABTS assay or inactive in the DPPH assay.

Table 1. Antioxidant activity of crude extracts of *C. sertularioides* expressed as the IC_{50} value (μg/mL).

Sample	ABTS	DPPH
Hexane	70.0 ± 11.5 ^{ab}	348.3 ± 82.2 ^{b}
Acetone	27.3 ± 6.1 ^{bc}	445.7 ± 59.4 ^{b}
Methanol	95.0 ± 16.3 ^{a}	1693.0 ± 43.1 ^{a}
Trolox	2.9 ± 0.1 ^{c}	4.8 ± 0.8 ^{c}

The values represent the mean of three independent determinations ± standard error. The different letters in the same column indicate a significant difference between the treatments in each assay ($p < 0.05$).

3.3. Cell Viability Assay

3.3.1. Crude Extracts

The crude extracts were evaluated at 100 and 200 μg/mL in cancerous and non-cancerous cell lines, to determine their effect on MTT reduction as an indicator of cellular metabolic activity and apparent viability (Table 2). The hexane extract produced the greatest reduction in MTT-derived metabolic activity, with apparent viability values of 10% and 18% in MDA-MB-231 and HeLa cells, respectively, at a concentration of 200 μg/mL. The acetone extract was also able to reduce the viability of the breast cancer cell line to 14% at

a concentration of 200 µg/mL. The methanol extract showed no significant effect at the tested concentrations.

Table 2. Apparent viability of human cell lines exposed to *C. sertularioides* extracts at different concentrations.

Extract	Dose (µg/mL)	Cell Line Viability (%)					
		MDA-MB-231	HCT116	22Rv1	HeLa	A549	ARPE-19
Hexane	200	10.0 ± 0.6 ^{a}	39.0 ± 13.3 ^{ab}	51.0 ± 7.7 ^{b}	18.0 ± 8.0 ^{ab}	50.0 ± 26.0 ^{ab}	79.0 ± 16.0 ^{bc}
	100	89.0 ± 11.9 ^{d}	92.0 ± 21.5 ^{cde}	99.0 ± 3.9 ^{cd}	94.0 ± 6.5 ^{cde}	106.0 ± 10.0 ^{bc}	109.0 ± 18.0 ^{cd}
Acetone	200	14.0 ± 6.1 ^{ab}	32.0 ± 21.3 ^{ab}	50.0 ± 4.6 ^{b}	56.0 ± 3.5 ^{bc}	54.0 ± 19.0 ^{ab}	50.0 ± 7.0 ^{ab}
	100	59.0 ± 6.0 ^{c}	66.0 ± 11.9 ^{bcd}	77.0 ± 2.8 ^{c}	72.0 ± 8.0 ^{c}	123.0 ± 23.0 ^{bc}	79.0 ± 10.0 ^{bc}
Methanol	200	96.0 ± 8.5 ^{d}	97.0 ± 11.9 ^{de}	114.0 ± 3.9 ^{de}	94.0 ± 4.5 ^{cde}	88.0 ± 5.0 ^{bc}	110.0 ± 7.0 ^{cd}
	100	95.0 ± 2.9 ^{d}	97.0 ± 5.6 ^{de}	108.0 ± 3.3 ^{de}	106.0 ± 7.5 ^{def}	160.0 ± 28.0 ^{bc}	111.0 ± 4.0 ^{cd}
Doxorubicin	200	35.0 ± 6.8 ^{bc}	55.0 ± 15.5 ^{abc}	40.0 ± 9.3 ^{b}	42.0 ± 9.0 ^{b}	27.0 ± 3.0 ^{a}	70.0 ± 6.0 ^{abc}
Cisplatin	200	14.0 ± 2.0 ^{ab}	27.0 ± 8.7 ^{a}	8.0 ± 0.5 ^{a}	10.0 ± 0.5 ^{a}	41.1 ± 2.0 ^{b}	29.0 ± 4.0 ^{a}

Values represent the mean of triplicate determinations ± standard error. The different letters in the same column indicate significant differences between the concentrations for each cell line ($p < 0.05$). Control cell cultures were incubated with DMSO and considered as 100% viability. ARPE-19, retinal pigment epithelial cells; A549, human lung adenocarcinoma cells; HeLa, human cervical adenocarcinoma cells; 22Rv1, human prostate carcinoma cells; HCT116, human colorectal carcinoma cells; MDA-MB-231, human invasive breast adenocarcinoma cells.

3.3.2. Selectivity Index of Crude Extracts

All tested cell lines were exposed to various concentrations of either hexane or acetone extracts and IC_{50} values and selectivity indices were calculated. The results are summarized in Table 3, which shows that the hexane extract exhibited the highest selectivity index toward the MDA-MB-231 cell line. Based on these results, this extract was selected for further purification and evaluation in this cell line. As the methanol extract did not show any effect on the tested cell lines, it was excluded from further analysis.

Table 3. Selectivity index of crude extracts from *C. sertularioides*.

Extract	MDA-MB-231	22Rv1	HeLa	HCT116	A549
Hexane	2.13	1.43	1.93	1.62	1.51
Acetone	1.66	1	0.85	1.35	0.97

3.3.3. Fractions

The hexane extract was selected for fractionation because it showed the highest exploratory selectivity index against MDA-MB-231 cells among the evaluated extract–cell line combinations, as shown in Table 3. Consequently, MDA-MB-231 cells were selected as the cancer cell model for the subsequent activity-guided evaluation. The hexane extract was fractionated by open-column chromatography, and the collected eluates were monitored under short- and long-wavelength UV light and grouped into 36 fractions according to similarities in their TLC profiles and Rf values. The amount obtained for each fraction ranged from 2.2 to 52.0 mg. The yields, calculated relative to the initial dry algal biomass used for extraction, ranged from 0.005% to 0.121%. The amounts, yields, and TLC Rf values of the 36 fractions are presented in Table S1.

All fractions were tested against the MDA-MB-231 cell line at a concentration of 100 µg/mL. Fractions 13, 15–17, and 19–24 reduced breast cancer cell viability down to <20% (Figure 1A). These 10 fractions were tested at 50 µg/mL to select the one with the highest activity (Figure 1B). Results show that fractions 15–17 and 20–23 decreased cell

viability to below 80%. Figure 1C shows that fractions 13, 15, 17, 23, and 24 did not markedly reduce the viability of ARPE-19 cells.

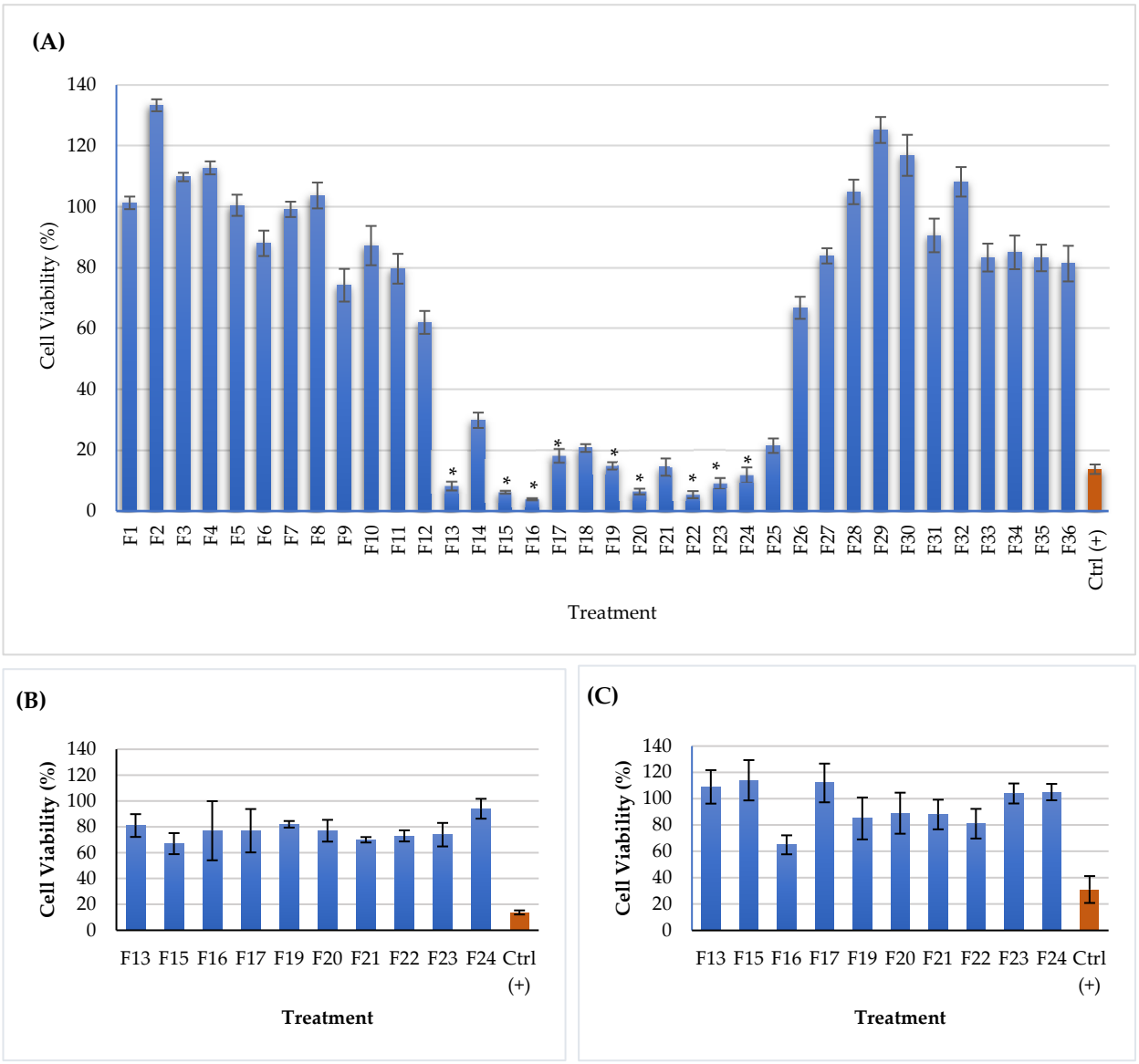

Figure 1. Effects of *C. sertularioides* fractions on the apparent viability of MDA-MB-231 and ARPE-19 cells. MDA-MB-231 cells were treated at (**A**) 100 µg/mL and (**B**) 50 µg/mL, whereas ARPE-19 cells were treated at (**C**) 50 µg/mL. Values represent the mean ± SE of three independent experiments. Asterisks indicate significant differences ($p < 0.05$). The positive control culture was treated with cisplatin (200 µg/mL) and the culture treated with DMSO was considered to represent 100% apparent viability.

3.3.4. IC_{50} and Selectivity Index of Fractions

Fractions that produced the greatest reductions in MTT-derived metabolic activity were selected for further analysis. IC_{50} values were determined in MDA-MB-231 and ARPE-19 cells, and exploratory selectivity indices were calculated (Table S2). Fractions 15 and 16 showed the highest SI values among the evaluated fractions. However, because ARPE-19 cells are not a tissue-matched non-cancerous counterpart of MDA-MB-231 cells, these values were used only as preliminary indicators for prioritizing fractions for subsequent analyses.

3.4. Fluorescence Cell Staining and Microscopy Assay

Nuclear and cytoskeletal staining was used to assess whether the compounds isolated from *C. sertularioides* modify cellular structure. MDA-MB-231 cells treated with fraction 15 displayed characteristics of apoptotic cells, with most exhibiting chromatin condensation and volume reduction; some showed membrane projections, protrusions, and chromatin fragmentation (Figure 2).

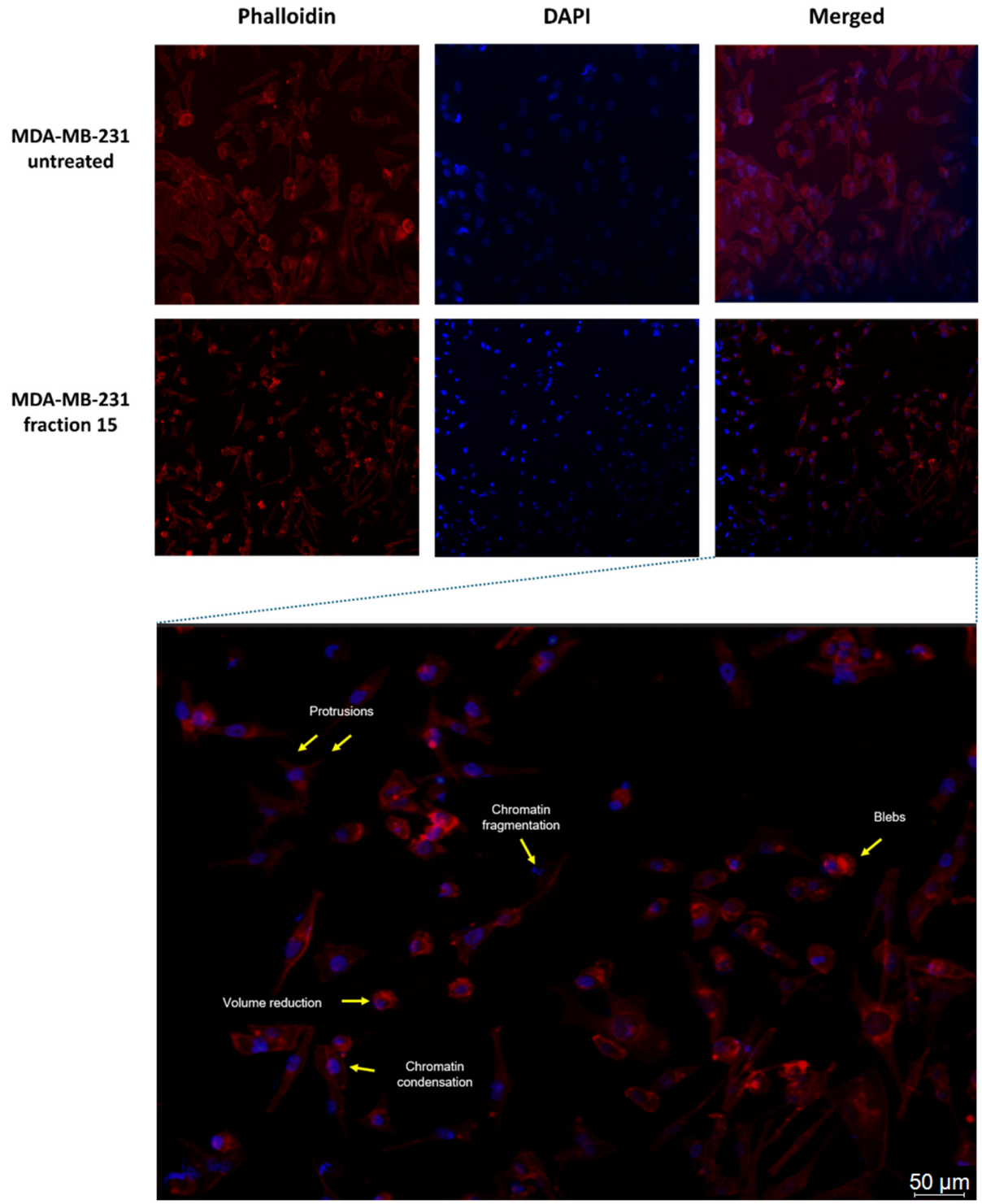

Figure 2. Fluorescence micrographs of untreated MDA-MB-231 cells (control) and cells treated with fraction 15 at its IC_{50}. Images were captured at 20× magnification. Cells were stained with DAPI to visualize nuclei and phalloidin to visualize the cytoskeleton. Scale bar = 50 µm.

3.5. Proton and Carbon Nuclear Magnetic Resonance Analysis

The acquired ^{1}H NMR spectra in $CDCl_3$ are shown in Figure S1. In fraction 15 (Figure S1A), the major component exhibits ^{1}H NMR signals at δ 8.09 (singlet, aromatic H), 4.29 (triplet, CH_2–O), 1.75 (multiplet, CH–CH_2), 1.50–1.20 (multiplet, aliphatic CH_2), and 1.02–0.85 ppm (multiplet, aliphatic CH_3). The ^{13}C NMR spectrum showed signals at δ 165.96, 134.23, 129.24, 67.59, 38.99, 30.66, 29.00, 23.98, 22.82, 14.15, and 11.20 ppm, consistent with those reported for bis(2-ethylhexyl) terephthalate. In fraction 16 (Figure S1B), terephthalate signals were predominant and bis(2-ethylhexyl) phthalate signals were present in a reduced proportion.

Based on its antiproliferative activity and selectivity index, fraction 15 was selected for additional chromatographic separation. This procedure yielded 35 subfractions, which were analyzed by UV–Vis spectroscopy and compared with the absorption profiles of the parent fraction and a commercial reference standard. Subfractions 1–10 exhibited absorption profiles similar to that of fraction 15, while showing a lower intensity of the signal associated with the reference standard. Therefore, these subfractions were pooled and designated SF1–10 for subsequent NMR analysis. In the ^{1}H NMR spectrum of SF1–10 (Figure S1C), terephthalate signals were markedly reduced, whereas the signals attributed to bis(2-ethylhexyl) phthalate are more clearly observed at δ 7.70 and 7.51 (doublets, aromatic H), 4.23 (triplet, CH_2–O), 1.70 (multiplet, CH–CH_2), 1.46–1.30 (multiplet), and 0.96–0.86 ppm (triplet, CH_3). In the expanded region from δ 9 to 2 ppm, minor component signals are visible. The signals at δ 4.05–4.40 ppm correspond to CH_2 groups bonded to electronegative atoms (present in terephthalate, phthalate, and glyceride moieties), those at δ 5.20–5.30 ppm correspond to unsaturated protons (–CH=CH–), those at δ 3.15–3.35 ppm are characteristic of glycerol, signals at δ 4.11 and 2.30–2.40 ppm correspond to CH_2 groups adjacent to unsaturated bonds, and the high-field region (δ 1.50–0.80 ppm) includes the CH_2 and CH_3 of aliphatic chains. These minor signals are consistent with those reported by Nieva-Echevarria et al. for 1-monolinolein and linoleic acid [26]. It was not possible to characterize the minor components by ^{13}C NMR because of their low concentration. The main compounds proposed from the NMR spectra are summarized in Table S3.

To assess whether the phthalate- and terephthalate-related signals detected in fraction 15 could have originated from either the hexane used during extraction or from the chromatographic purification procedure, five concentrated hexane samples representing stages of the procedure were analyzed by ^{1}H NMR. No signals were detected in the aromatic region of the ^{1}H NMR spectra, and only the characteristic resonances of hexane were observed (Figure S2). These results reduced the likelihood that the analyzed solvents and silica gel were the source of the aromatic signals observed in fraction 15.

Furthermore, to assess whether the antiproliferative effect of fraction 15 could be associated with the proposed phthalate derivative, a commercial phthalate standard (bis(2-ethylhexyl) phthalate) was evaluated in ARPE-19 and MDA-MB-231 cells (Figure S3). The phthalate standard did not induce a marked or concentration-dependent reduction in cell viability at concentrations ranging from 12.5 to 400 μg/mL in ARPE-19 cells (Figure S3A). In MDA-MB-231 cells, cell viability ranged from approximately 80 to 105% (Figure S3B), whereas fraction 15 exhibited an IC_{50} of approximately 55 μg/mL. These results indicate that the antiproliferative activity of fraction 15 cannot be attributed solely to DEHP, since the commercial standard did not reproduce the concentration-dependent reduction in MDA-MB-231 cell viability observed for fraction 15. Therefore, the activity may involve other constituents of the fraction or combined effects among its components.

Further isolation and structural confirmation of the individual constituents will be required to identify the compound or compounds responsible for this activity.

4. Discussion

Caulerpa sertularioides is native to Mexico and appears in both the Gulf of Mexico and the Pacific Ocean [21]. In the present study, specimens were collected along the coast of Sonora, northern Mexico. Seaweed chemical composition and extraction yield may vary depending on several factors, including biogeographic region [27]. The moisture content and extraction yields obtained in this study were comparable to those reported by Osuna-Ruíz et al. for *C. sertularioides* collected in Sinaloa [18,28]. Belkacemi et al. reported hexane and methanol extraction yields of 3.9% and 10.2%, respectively, from *C. racemosa* [29], while Mehra et al. reported an 8% methanol extraction yield for *C. taxifolia* [30]. Differences among studies may reflect species-specific and environmental factors; nevertheless, extraction yields generally increased with solvent polarity.

Antioxidants play an essential role in protecting cells against oxidative damage caused by reactive oxygen species (ROS) generated during cellular metabolism [31]. In the present study, the acetone extract had potent antioxidant capacity as assessed by the ABTS assay, whereas the hexane and methanol extracts showed moderate activity.

Comparable ABTS antioxidant activity has been reported for Caulerpa species, including hexane, acetone, and methanol extracts of *C. sertularioides* with values below 10 vitamin C equivalents [18], an aqueous extract of *C. sertularioides* with an EC_{50} of 11 μg/mL [14], and hexane and methanol extracts of *C. racemosa* with EC_{50} values of 3540 μg/mL [29]. In contrast, all extracts evaluated in the present study showed weak DPPH activity (IC_{50} > 250 μg/mL). Similar low activity has been reported for several Caulerpa species evaluated using the DPPH method, including methanol and acetone extracts of *C. sertularioides*, with EC_{50} of 116,400 μg/mL and 150,600 μg/mL, respectively [18], and for hexane and methanol of *C. racemosa* (11,070 μg/mL and 42,060 μg/mL, respectively) [29]. Lower EC_{50} values have also been reported for aqueous and protein extracts of *C. sertularioides* (10 and 181 μg/mL, respectively) [14,32], whereas polysaccharides from *C. taxifolia* reduced DPPH radical activity by 16% at 1000 μg/mL [33].

Previous studies have reported antioxidant compounds in *Caulerpa* extracts, including flavonoids, chlorophylls, phenolic compounds, carotenoids, and lectins [18,28,29,32,33]. Natural polyphenols are recognized for their antioxidant, anti-inflammatory, cytotoxic, antineoplastic, and immunomodulatory properties and have been proposed as chemopreventive and chemotherapeutic agents [34–36]. Certain flavonoids can also modulate cancer-related signaling pathways [37], while pigments, particularly carotenoids, have been widely associated with antioxidant and anticancer activities [18,38].

The MTT assay estimates cellular metabolic activity through the enzymatic reduction of MTT to formazan by metabolically active cells. Therefore, the reductions observed in the present study should be interpreted as decreases in metabolic activity and apparent cell viability rather than as direct evidence of cytotoxicity or cell death. Changes in MTT reduction may result from a decrease in cell number, suppression of cellular metabolism, or loss of viability, which cannot be distinguished by this assay alone.

The hexane and acetone extracts reduced MTT-derived metabolic activity in all evaluated cancer cell lines, although the magnitude of this effect varied among them. These differences may reflect variations in tissue origin, metabolic characteristics, proliferation rates, membrane transport, and molecular profile, which can influence compound uptake, metabolism, and intracellular targets. MDA-MB-231 and HeLa cells showed the greatest reductions in metabolic activity; however, because the underlying mechanisms were not investigated, these findings should be interpreted as a preliminary indication of differential sensitivity rather than evidence of a tissue-specific effect.

The effects observed in breast cancer cells were comparable to those reported for other Caulerpa species by Mehra et al. (IC_{50} of 190 μg/mL) and Sanger et al. (IC_{50} of 24 μg/mL) [30,39].

The biological activity of fractions obtained by open-column chromatography and monitored by TLC of *C. sertularioides* was further assessed. Several fractions reduced the apparent viability of MDA-MB-231 cells, with fraction 15 exhibiting the highest selectivity index (3.75).

Similarly, Nurkolis et al. reported selectivity indices of 17.9 and 14.3 for hexane extracts of *C. lentillifera* against MDA-MB-231 and MCF-7 cells, respectively [40]. Dissanayake et al. reported selectivity indices of 4.49 and 2.48 for a crude polyphenolic extract of *C. racemosa* against KAIMRC1 and MDA-MB-231, respectively [24]. The selectivity indices obtained in the present study should be interpreted cautiously because ARPE-19 was the only non-cancerous cell line evaluated and is not tissue-matched to the cancer cell lines. Therefore, these values provide only a preliminary indication of differential sensitivity. Future studies should include tissue-matched non-cancerous models, particularly a non-tumorigenic mammary epithelial cell line for comparison with MDA-MB-231.

Apoptosis is essential for cellular homeostasis in multicellular organisms and can be triggered by both intra- and extracellular signals [41]. This process is characterized by distinct morphological changes, including cell shrinkage, membrane blebbing, chromatin condensation, DNA fragmentation, and the formation of apoptotic bodies [42,43]. In addition, early activation of caspases may lead to the formation of membrane protrusions or microtubule-associated spikes, which have been associated with exposure to genotoxic compounds [44].

In the present study, fraction 15 induced morphological changes in MDA-MB-231 cells consistent with apoptosis, including cell contraction, nuclear condensation, and fragmentation. Similar alterations have been reported for ethanolic extracts of *C. sertularioides* in SKLU-1 lung cancer cell line [19], methanol extracts of *C. racemosa* and *C. scalpelliformis* [45], compounds extracted from *C. lentillifera* in MCF-7 breast cancer cells [46], and ethanolic extracts of *C. racemosa* in HeLa cervical cancer cells [47].

Fraction 15 exhibited the highest biological activity against MDA-MB-231 and was therefore selected for structural characterization. The ^{1}H and ^{13}C NMR spectral signals were consistent with those reported for bis(2-ethylhexyl) terephthalate (DEHT) [48].

Phthalates and related plasticizers have been reported in marine environments and organisms, including macroalgae, where their presence may result from environmental contamination and bioaccumulation [49]. Some macroalgal species can accumulate specific plasticizers from the surrounding medium under controlled conditions [50]. In addition, the possible natural production of some phthalates by macroalgae has been proposed based on comparisons of the natural abundance of ^{14}C in compounds isolated from biological sources and in industrial products [51].

Because DEHP and DEHT are also common laboratory contaminants [52,53], the possibility that the signals detected in fraction 15 originated from reagents or materials used during extraction and purification was carefully considered. ^{1}H NMR analyses of the different hexane sources and of hexane passed through the silica gel column did not show detectable aromatic signals attributable to these compounds. Although these controls reduced the likelihood that the analyzed solvents and silica gel were the source of the detected signals, they do not completely exclude incidental contamination from other materials used during sample handling.

The commercial DEHP standard did not reproduce the antiproliferative effect observed for fraction 15 in MDA-MB-231 cells, indicating that DEHP alone is unlikely to account for the observed activity. However, because the individual constituents could not be completely

isolated, the active compound or compounds, and possible combined effects among the components, remain to be determined.

Fraction 15 contained signals consistent with linoleic acid and 1-monolinolein, although in lower proportions. Ogata et al. reported that linoleic acid suppressed energy metabolism in cancer cells, inducing a quiescent metabolic state and cellular dormancy [54]. Cancer dormancy has been associated with late recurrence, metastasis, therapeutic resistance and immune evasion [55].

García et al. reported that linoleic acid promoted extracellular vesicle release from MDA-MB-231 cells, enhancing angiogenesis in human umbilical vein endothelial cells [56]. These findings suggest that linoleic acid may exert complex and context-dependent effects in cancer biology. Therefore, the contribution of linoleic acid to the antiproliferative activity observed in fraction 15 cannot be directly inferred and may involve concentration-dependent mechanisms or interactions with other metabolites.

Vu et al. reported cytotoxic activity of 1-monolinolein against lung cancer [57]. Network pharmacology and molecular docking analyses also report favorable interactions of this compound with seven colon cancer-related targets [58]. In addition, Berdesh et al. demonstrated cytotoxic effects of 1-monolinolein against prostate, colon, and breast cancer cell lines [59].

The lipophilic compounds detected in fraction 15 may contribute to the observed antiproliferative effects through mechanisms involving cell-cycle arrest and cell death. However, because these compounds were detected within a complex mixture, their individual contribution to biological activity cannot be established. Further purification, quantitative analysis, and mechanistic evaluation are therefore required to clarify their specific role in the observed activity.

Overall, this study expands current knowledge of the bioactive potential of marine macroalgae from the Mexican Pacific. By integrating chemical characterization and biological evaluation, it provides new evidence of the antiproliferative activity of lipophilic fractions from *C. sertularioides*, a comparatively underexplored species. The tentative detection of compounds previously associated with cytotoxic activity further supports the pharmacological relevance of this macroalga. However, additional studies are required to isolate the active constituents, confirm their structures, and clarify the mechanisms underlying the observed effects.

5. Conclusions

The present study showed that lipophilic extracts obtained from *C. sertularioides* exhibit antiproliferative activity against breast cancer cells, with fraction 15 displaying the highest antiproliferative activity and selectivity among the evaluated fractions. NMR analysis revealed signals tentatively assigned to 1-monolinolein, linoleic acid, bis(2-ethylhexyl) phthalate, and a terephthalate-related compound. The origin of the phthalate- and terephthalate-related signals could not be conclusively established; however, the commercial DEHP standard did not reproduce the antiproliferative effect of fraction 15, indicating that DEHP alone is unlikely to account for the observed activity. MDA-MB-231 cells treated with fraction 15 exhibited morphological alterations consistent with apoptosis, including cell shrinkage, chromatin condensation, and nuclear fragmentation.

These findings support the potential of *C. sertularioides* as a source of fractions containing compounds of pharmacological interest. However, given the chemical complexity of the analyzed fraction, and the inability to completely isolate the individual constituents, further purification, quantitative characterization, and mechanistic studies are required to confirm the proposed compounds, determine their origin, identify the constituents responsible for the antiproliferative activity, and elucidate molecular pathways involved.

Supplementary Materials: The following supporting information can be downloaded at: https://www.mdpi.com/article/10.3390/scipharm94030079/s1.

Author Contributions: Conceptualization, C.M.L.-S., R.R.-P. and I.O.-R.; methodology, E.S.-P., M.G.B.-Z., H.d.C.S.-O. and M.P.-J.; formal analysis, E.S.-P., M.P.-J., C.M.L.-S. and H.d.C.S.-O.; investigation, E.S.-P., C.M.L.-S., E.M.A.-M., M.G.B.-Z. and R.R.-P.; writing—original draft preparation, E.S.-P. and E.M.A.-M.; writing—review and editing, R.R.-P., H.d.C.S.-O., I.O.-R. and C.M.L.-S.; project administration, M.P.-J. and C.M.L.-S.; funding acquisition, C.M.L.-S. All authors have read and agreed to the published version of the manuscript.

Funding: This research received no external funding.

Institutional Review Board Statement: Not applicable.

Informed Consent Statement: Not applicable.

Data Availability Statement: All relevant data supporting the findings of this study are contained within this article.

Acknowledgments: The authors thank the cancer cell culture laboratory at the University of Sonora for donating the cell lines used in this work. The authors thank SECITHI, which contributed to a postgraduate scholarship (CVU 270619).

Conflicts of Interest: The authors declare no conflicts of interest.

Abbreviations

The following abbreviations are used in this manuscript:

MTT	3-(4,5-dimethylthiazol-2-yl)-2,5-diphenyltetrazolium bromide
ABTS	2′-azino-bis(3-ethylbenzothiazolin-6-sulfonic acid)
DPPH	2,2-diphenyl-1-picrylhydrazyl
TLC	thin-layer chromatography
NMR	nuclear magnetic resonance
IC50	half-maximal inhibitory concentration
SI	selectivity index

References

1. National Cancer Institute. Understanding Cancer. Available online: https://www.cancer.gov/about-cancer/understanding/what-is-cancer (accessed on 30 June 2025).
2. Sung, H.; Filho, A.M.; Laversanne, M.; Ferlay, J.; Siegel, R.; Soerjomataram, I.; Jemal, A.; Bray, F. Global cancer statistics 2024: GLOBOCAN estimates of incidence and mortality worldwide for 34 cancers in 186 countries. *CA Cancer J. Clin.* **2026**, *76*, e70090. [CrossRef] [PubMed]
3. Ling, L. Inequality in breast cancer: Global statistics from 2022 to 2050. *Breast* **2025**, *79*, 103851. [CrossRef] [PubMed]
4. World Health Organization. Breast Cancer. Available online: https://www.who.int/news-room/fact-sheets/detail/cancer (accessed on 3 February 2025).
5. Liu, Y.; Wang, X.; He, D.; Cheng, Y. Protection against chemotherapy- and radiotherapy-induced side effects: A review based on the mechanisms and therapeutic opportunities of phytochemicals. *Phytomedicine* **2021**, *80*, 153402. [CrossRef] [PubMed]
6. Khan, S.; Kaneez, F.; Shariqa, A.; Fayaz, M. Unveiling the mechanisms and challenges of cancer drug resistance. *Cell Commun. Signal.* **2024**, *22*, 109. [CrossRef] [PubMed]
7. Gu, Y.; Yang, R.; Zhang, Y.; Guo, M.; Takehiro, K.; Zhan, M.; Yang, L.; Wang, H. Molecular mechanisms and therapeutic strategies in overcoming chemotherapy resistance in cancer. *Mol. Biomed.* **2025**, *6*, 2. [CrossRef] [PubMed]
8. Wei, J.R.; Lu, M.Y.; Wei, T.H.; Fleishman, J.; Yu, H.; Chen, X.L.; Kong, X.T.; Sun, S.L.; Li, N.G.; Yang, Y.; et al. Overcoming cancer therapy resistance: From drug innovation to therapeutics. *Drug Resist. Updates* **2025**, *81*, 101229. [CrossRef] [PubMed]
9. Haque, A.; Brazeau, D.; Amin, A. Perspectives on natural compounds in chemoprevention and treatment of cancer: An update with new promising compounds. *Eur. J. Cancer* **2021**, *149*, 165–183. [CrossRef] [PubMed]
10. Mbaoji, F.; Nweze, J.; Yang, L.; Huang, Y.; Huang, S.; Onwuka, A.; Peter, I.; Mbaoji, C.; Jiang, M.; Zhang, Y.; et al. Novel Marine Secondary Metabolites Worthy of Development as Anticancer Agents: A Review. *Molecules* **2021**, *26*, 5769. [CrossRef] [PubMed]

11. Dayanidhi, D.; Thomas, B.; Osterberg, J.; Vuong, M.; Vargas, G.; Kwartler, S.; Schmaltz, E.; Dunphy-Daly, M.; Schultz, T.; Rittschof, D.; et al. Exploring the Diversity of the Marine Environment for New Anti-cancer Compounds. *Front. Mar. Sci.* **2021**, *7*, 614766. [CrossRef]
12. Minhas, L.; Kaleem, M.; Umer, H.; Kausar, F.; Waqar, R.; Bhatti, T.; Aziz, S.; Jung, D.; Mumtaz, A. Algae-derived bioactive compounds as potential pharmaceuticals for cancer therapy: A comprehensive review. *Algal Res.* **2024**, *78*, 103396. [CrossRef]
13. Warnasooriya, V.; Gunawardena, S.; Weththasinghe, P.; Jayawardana, B.; Qader, M.; Liyanage, R. Nutritional Properties, Antioxidant Activity, and Heavy Metal Accumulation in Selected Marine Macro-Algae Species of Sri Lanka. *Nutraceuticals* **2024**, *4*, 50–64. [CrossRef]
14. Anjali, R.; Palanisamy, S.; Vinosha, M.; Selvi, A.M.; Sathiyaraj, G.; Marudhupandi, T.; Mohandoss, S.; Prabhu, N.M.; You, S.G. Fabrication of silver nanoparticles from marine macro algae *Caulerpa sertularioides*: Characterization, antioxidant and antimicrobial activity. *Process Biochem.* **2022**, *121*, 601–618. [CrossRef]
15. Frazzini, S.; Rossi, L. Anticancer Properties of Macroalgae: A Comprehensive Review. *Mar. Drugs* **2025**, *23*, 70. [CrossRef] [PubMed]
16. Kanegawa, K.; Harada, H.; Myouga, H.; Katakura, Y.; Shirahata, S.; Kamei, Y. Telomerase inhibiting activity in vitro from natural resources, marine algae extracts. *Cytotechnology* **2000**, *33*, 221–227. [CrossRef] [PubMed]
17. Costa, L.S.; Fidelis, G.P.; Cordeiro, S.L.; Oliveira, R.M.; Sabry, D.A.; Câmara, R.B.G.; Nobre, L.T.D.B.; Costa, M.S.S.P.; Almeida-Lima, J.; Farias, E.H.C.; et al. Biological activities of sulfated polysaccharides from tropical seaweeds. *Biomed. Pharmacother.* **2010**, *64*, 21–28. [CrossRef] [PubMed]
18. Osuna-Ruiz, I.; López-Saiz, C.; Burgos-Hernández, A.; Velázquez, C.; Nieves-Soto, M.; Hurtado-Oliva, M. Antioxidant, antimutagenic and antiproliferative activities in selected seaweed species from Sinaloa, Mexico. *Pharm. Biol.* **2016**, *54*, 2196–2210. [CrossRef] [PubMed]
19. Agena, R.; Cortés-Sánchez, A.D.J.; Hernández-Sánchez, H.; Álvarez-Salas, L.M.; Martínez-Rodríguez, O.P.; García, V.H.R.; Jaramillo Flores, M.E. Pro-Apoptotic Activity and Cell Cycle Arrest of *Caulerpa sertularioides* against SKLU-1 Cancer Cell in 2D and 3D Cultures. *Molecules* **2023**, *28*, 4361. [CrossRef] [PubMed]
20. Sivakumar, V.; Palanisamy, S.; Rajasekar, P.; Solomon, J.; Pandi, T.; Manoharan, V.; Ravichandran, A.; Mohandoss, S.; Marudhupandi, T.; SangGuanYou; et al. Biogenic gold nanoparticles synthesized from *Caulerpa sertularioides*: A green approach for antioxidant, antibacterial and anticancer applications. *Bioorg. Chem.* **2025**, *165*, 108963. [CrossRef] [PubMed]
21. Norris, J.N. *Marine Algae of the Northern Gulf of California: Chlorophyta and Phaeophyceae*, 1st ed.; Smithsonian Institution Scholarly Press: Washington, DC, USA, 2010; pp. 95–98.
22. Trujillo-Ruiz, H.E.; López-Saiz, C.M.; García-Alegría, A.M.; Osuna-Ruiz, I.; Santacruz-Ortega, H.D.C.; Meza-Montenegro, M.M.; Maldonado-Escalante, J.F.; Cruz-Ramirez, S.G.; Burgos-Hernández, A. Detection and partial characterization of antimutagenic compounds from white shrimp (*Litopenaeus vannamei*) cephalothorax. *CyTA—J. Food* **2024**, *22*, 2315990. [CrossRef]
23. Mosmann, T. Rapid colorimetric assay for cellular growth and survival: Application to proliferation and cytotoxicity assays. *J. Immunol. Methods* **1983**, *65*, 55–63. [CrossRef] [PubMed]
24. Dissanayake, I.H.; Bandaranayake, U.; Keerthirathna, L.R.; Manawadu, C.; Silva, R.M.; Mohamed, B.; Ali, R.; Peiris, D.C. Integration of in vitro and in-silico analysis of *Caulerpa racemosa* against antioxidant, antidiabetic, and anticancer activities. *Sci. Rep.* **2022**, *12*, 20848. [CrossRef] [PubMed]
25. Van Vuuren, R.J.; Botes, M.; Jurgens, T.; Joubert, A.M.; Van Den Bout, I. Novel sulphamoylated 2-methoxy estradiol derivatives inhibit breast cancer migration by disrupting microtubule turnover and organization. *Cancer Cell Int.* **2019**, *19*, 1. [CrossRef] [PubMed]
26. Nieva-Echevarría, B.; Goicoechea, E.; Manzanos, M.J.; Guillén, M.D. A method based on 1H NMR spectral data useful to evaluate the hydrolysis level in complex lipid mixtures. *Food Res. Int.* **2014**, *66*, 379–387. [CrossRef]
27. McKinney, R.; Cunningham, E.; Burton, J.; Kraan, S.; Dick, J.; Walsh, P. Fine-scale biochemical variation in *Fucus serratus* (Phaeophyceae): Point sampling vs bulk samples and implications for industrial applications. *J. Appl. Phycol.* **2026**, *38*, 601–612. [CrossRef]
28. Osuna-Ruiz, I.; Nieves-Soto, M.; Manzano-Sarabia, M.M.; Hernández-Garibay, E.; Lizardi-Mendoza, J.; Burgos-Hernández, A.; Hurtado-Oliva, M.Á. Gross chemical composition, fatty acids, sterols, and pigments in tropical seaweed species off Sinaloa, Mexico. *Cienc. Mar.* **2019**, *45*, 101–120. [CrossRef]
29. Belkacemi, L.; Belalia, M.; Djendara, A.; Bouhadda, Y. Antioxidant and antibacterial activities and identification of bioactive compounds of various extracts of *Caulerpa racemosa* from Algerian coast. *Asian Pac. J. Trop. Biomed.* **2020**, *10*, 87–94. [CrossRef]
30. Mehra, R.; Bhushan, S.; Bast, F.; Singh, S. Marine macroalga Caulerpa: Role of its metabolites in modulating cancer signaling. *Mol. Biol. Rep.* **2019**, *46*, 3545–3555. [CrossRef] [PubMed]
31. Gâman, M.-A.; Epîngeac, M.E.; Diaconu, C.C.; Gâman, A.M. Evaluation of oxidative stress levels in obesity and diabetes by the free oxygen radical test and free oxygen radical defence assays and correlations with anthropometric and laboratory parameters. *World J. Diabetes* **2020**, *11*, 193–201. [CrossRef] [PubMed]

32. Sanniyasi, E.; Gopal, R.K.; Raj, P.P.; Shanmugavel, A.K. Anti-inflammatory, remorin-like protein from green marine Macroalga *Caulerpa sertularioides* (S.G.Gmel.) M.Howe. *Heliyon* **2023**, *9*, 19239. [CrossRef] [PubMed]
33. Bayro, A.M.; Manlusoc, J.K.; Alonte, R.; Caniel, C.; Conde, P.; Embralino, C. Preliminary Characterization, Antioxidant and Antiproliferative Properties of Polysaccharide from *Caulerpa taxifolia*. *Pharm. Sci. Res.* **2021**, *8*, 30–36. [CrossRef]
34. Gomes, D.L.; Telles, C.B.S.; Costa, M.S.S.P.; Almeida-Lima, J.; Costa, L.S.; Keesen, T.S.L.; Rocha, H.A.O. Methanolic extracts from brown seaweeds *Dictyota cilliolata* and *Dictyota menstrualis* induce apoptosis in human cervical adenocarcinoma HeLa cells. *Molecules* **2015**, *20*, 6573–6591. [CrossRef] [PubMed]
35. Tenorio-Rodriguez, P.A.; Méndez-Rodríguez, L.C.; Serviere-Zaragoza, E.; O'Hara, T.; Zenteno-Savín, T. Antioxidant Substances and Trace Element Content in Macroalgae from a Subtropical Lagoon in the West Coast of the Baja California Peninsula. *Vitam. Trace Elem.* **2013**, *02*, 1000108.
36. Davatgaran-Taghipour, Y.; Masoomzadeh, S.; Farzaei, M.H.; Bahramsoltani, R.; Karimi-Soureh, Z.; Rahimi, R.; Abdollahi, M. Polyphenol nanoformulations for cancer therapy: Experimental evidence and clinical perspective. *Int. J. Nanomed.* **2017**, *12*, 2689–2702. [CrossRef] [PubMed]
37. Ponte, L.G.S.; Pavan, I.C.B.; Mancini, M.C.S.; Da Silva, L.G.S.; Morelli, A.P.; Severino, M.B.; Rosangela Maria Neves Bezerra, R.M.; Simabuco, F.M. The hallmarks of flavonoids in cancer. *Molecules* **2021**, *26*, 2029. [CrossRef] [PubMed]
38. Rowles, J.L.; Erdman, J.W. Carotenoids and their role in cancer prevention. *BBA—Mol. Cell Biol. Lipids* **2020**, *1865*, 158613. [CrossRef] [PubMed]
39. Sanger, G.; Wonggo, D.; Taher, N.; Dotulong, V.; Setiawan, A.A.; Permatasari, H.K.; Maulana, S.; Nurkolis, F.; Apollinaire Tsopmo, A.; Kim, B. Green seaweed *Caulerpa racemosa*—Chemical constituents, cytotoxicity in breast cancer cells and molecular docking simulation. *J. Agric. Food Res.* **2023**, *12*, 100621. [CrossRef]
40. Nurkolis, F.; Taslim, N.A.; Qhabibi, F.R.; Kang, S.; Moon, M.; Choi, J.; Park, M.N.; Mayulu, N.; Kim, B. Ulvophyte Green Algae *Caulerpa lentillifera*: Metabolites Profile and Antioxidant, Anticancer, Anti-Obesity, and In Vitro Cytotoxicity Properties. *Molecules* **2023**, *28*, 1365. [CrossRef] [PubMed]
41. Jan, R.; Chaudhry, G.E.S. Understanding apoptosis and apoptotic pathways targeted cancer therapeutics. *Adv. Pharm. Bull.* **2019**, *9*, 205–218. [CrossRef] [PubMed]
42. Mills, J.C.; Stone, N.L.; Pittman, R.N. Extranuclear apoptosis: The role of the cytoplasm in the execution phase. *J. Cell Biol.* **1999**, *146*, 703–707. [PubMed]
43. Oropesa-Ávila, M.; Andrade-Talavera, Y.; Garrido-Maraver, J.; Cordero, M.D.; De La Mata, M.; Cotán, D.; Paz, M.V.; Pavo'n, A.D.; Alcocer-Gomez, E.; de Lavera, I.; et al. Stabilization of apoptotic cells: Generation of zombie cells. *Cell Death Dis.* **2014**, *5*, 1369. [CrossRef] [PubMed]
44. Povea-Cabello, S.; Oropesa-Ávila, M.; de la Cruz-Ojeda, P.; Villanueva-Paz, M.; De La Mata, M.; Suárez-Rivero, J.M.; Álvarez-Córdoba, M.; Villalón-García, I.; Cotán, D.; Ybot-González, P.; et al. Dynamic reorganization of the cytoskeleton during apoptosis: The two coffins hypothesis. *Int. J. Mol. Sci.* **2017**, *18*, 2393. [CrossRef] [PubMed]
45. Tanna, B.; Yadav, S.; Mishra, A. Anti-proliferative and ROS-inhibitory activities reveal the anticancer potential of Caulerpa species. *Mol. Biol. Rep.* **2020**, *47*, 7403–7411. [CrossRef] [PubMed]
46. Maeda, R.; Ida, T.; Ihara, H.; Sakamoto, T. Induction of apoptosis in MCF-7 cells by β-1,3-xylooligosaccharides prepared from *Caulerpa lentillifera*. *Biosci. Biotechnol. Biochem.* **2012**, *76*, 1032–1034. [CrossRef] [PubMed]
47. Permatasari, H.K.; Wewengkang, D.S.; Tertiana, N.I.; Muslim, F.Z.; Yusuf, M.; Baliulina, S.O.; Daud, V.P.A.; Setiawan, A.A.; Nurkolis, F. Anti-cancer properties of *Caulerpa racemosa* by altering expression of Bcl-2, BAX, cleaved caspase 3 and apoptosis in HeLa cancer cell culture. *Front. Oncol.* **2022**, *14*, 176–184. [CrossRef] [PubMed]
48. Kdimy, A.; Kim, S.J.; Ali, Z.; Khan, M.I.H.; Tripathi, S.K.; El Hajjaji, S.; Le, H.V. Isolation of Two Plasticizers, Bis(2-ethylhexyl) Terephthalate and Bis(2-ethylhexyl) Phthalate, from *Capparis spinosa* L. Leaves. *Chem. Biodivers.* **2023**, *20*, 202300903. [CrossRef] [PubMed]
49. Vieira, M.G.A.; Da Silva, M.A.; Dos Santos, L.O.; Beppu, M.M. Natural-based plasticizers and biopolymer films: A review. *Eur. Polym. J.* **2011**, *47*, 254–263. [CrossRef]
50. Savoca, D.; Lo Coco, R.; Melfi, R.; Pace, A. Uptake and photoinduced degradation of phthalic acid esters (PAEs) in Ulva lactuca highlight its potential application in environmental bioremediation. *Environ. Sci. Pollut. Res. Int.* **2022**, *29*, 90887–90897. [CrossRef] [PubMed]
51. Namikoshi, M.; Fujiwara, T.; Nishikawa, T.; Ukai, K. Natural Abundance 14C Content of Dibutyl Phthalate (DBP) from Three Marine Algae. *Mar. Drugs* **2006**, *4*, 290–297. [CrossRef]
52. Nguyen, T.B.T.; Nguyen, L.N.; Vo, T.N. Bis(2-Ethylhexyl) Terephthalate from Olax Imbricata, Natural Substance or Artifact? *J. Tech. Educ. Sci.* **2023**, *77*, 56–62. [CrossRef]
53. Iannone, A.; Di Fiore, C.; Carriera, F.; Avino, P.; Stillittano, V. Phthalates: The Main Issue in Quality Control in the Beverage Industry. *Separations* **2024**, *11*, 133. [CrossRef]

54. Ogata, R.; Mori, S.; Kishi, S.; Sasaki, R.; Iwata, N.; Ohmori, H.; Sasaki, T.; Nishiguchi, Y.; Nakashima, C.; Goto, K.; et al. Linoleic Acid Upregulates Microrna-494 to Induce Quiescence in Colorectal Cancer. *Int. J. Mol. Sci.* **2022**, *23*, 225. [CrossRef] [PubMed]
55. Dalla, E.; Sreekumar, A.; Aguirre-Ghiso, J.A.; Chodosh, L.A. Dormancy in Breast Cancer. *Cold Spring Harb. Perspect. Med.* **2023**, *13*, a041331. [CrossRef] [PubMed]
56. Garcia-Hernandez, A.; Leal-Orta, E.; Ramirez-Ricardo, J.; Cortes-Reynosa, P.; Thompson-Bonilla, R.; Salazar, E.P. Linoleic acid induces secretion of extracellular vesicles from MDA-MB-231 breast cancer cells that mediate cellular processes involved with angiogenesis in HUVECs. *Prostaglandins Other Lipid Mediat.* **2021**, *153*, 106519. [CrossRef] [PubMed]
57. Vu, H.; Nguyen, D.; Nguyen, H.; Chu, H.; Chu, S.; Chau, M.; Phi, Q. Antimicrobial and Cytotoxic Properties of Bioactive Metabolites Produced by Streptomyces cavourensis YBQ59 Isolated from Cinnamomum cassia Prels in Yen Bai Province of Vietnam. *Curr. Microbiol.* **2018**, *75*, 1247–1255. [CrossRef] [PubMed]
58. Zhang, M.M.; Wang, D.; Lu, F.; Zhao, R.; Ye, X.; He, L.; Ai, L.; Wu, C.J. Identification of the active substances and mechanisms of ginger for the treatment of colon cancer based on network pharmacology and molecular docking. *BioData Min.* **2021**, *14*, 1. [CrossRef] [PubMed]
59. Berdesh, T.; Çakir, C.; Çam, D.; Tuna, K.; Yeskaliyeva, B.; Öztürk, M. Determination of Cytotoxic Compounds of Lepista personata (Fr.) Cooke by Gas Chromatography-Mass Spectrometry (GC-MS) and Chemometrics. *Anal. Lett.* **2024**, *58*, 2007–2018. [CrossRef]